

Branching ratios and direct CP asymmetries in $D \rightarrow PP$ decaysHsiang-nan Li,^{1,2,3} Cai-Dian Lu,⁴ and Fu-Sheng Yu^{4,5}¹*Institute of Physics, Academia Sinica, Taipei, Taiwan 115, Republic of China*²*Department of Physics, National Cheng-Kung University, Tainan, Taiwan 701, Republic of China*³*Department of Physics, National Tsing-Hua University, Hsin-Chu, Taiwan 300, Republic of China*⁴*Institute of High Energy Physics and Theoretical Physics Center for Science Facilities, Chinese Academy of Sciences, Beijing 100049, People's Republic of China*⁵*Laboratoire de l'Accélérateur Linéaire, Université Paris-Sud 11, CNRS/IN2P3(UMR 8607) 91405 Orsay, France*

(Received 28 April 2012; published 27 August 2012)

We propose a theoretical framework for analyzing two-body nonleptonic D meson decays, based on the factorization of short-distance (long-distance) dynamics into Wilson coefficients (hadronic matrix elements of four-fermion operators). The parametrization of hadronic matrix elements in terms of several nonperturbative quantities is demonstrated for the $D \rightarrow PP$ decays, P denoting a pseudoscalar meson. We consider the evolution of Wilson coefficients with energy release in individual decay modes, and the Glauber strong phase associated with the pion in nonfactorizable annihilation amplitudes, that is attributed to the unique role of the pion as a Nambu-Goldstone boson and a quark-antiquark bound state simultaneously. The above inputs improve the global fit to the branching ratios involving the η' meson and resolve the long-standing puzzle from the $D^0 \rightarrow \pi^+ \pi^-$ and $D^0 \rightarrow K^+ K^-$ branching ratios, respectively. Combining short-distance dynamics associated with penguin operators and the hadronic parameters determined from the global fit to branching ratios, we predict direct CP asymmetries, to which the quark loops and the scalar penguin annihilation give dominant contributions. In particular, we predict $\Delta A_{CP} \equiv A_{CP}(K^+ K^-) - A_{CP}(\pi^+ \pi^-) = -1.00 \times 10^{-3}$, lower than the LHCb and CDF data.

DOI: [10.1103/PhysRevD.86.036012](https://doi.org/10.1103/PhysRevD.86.036012)

PACS numbers: 11.30.Er, 12.39.St, 13.25.Ft

I. INTRODUCTION

Two-body nonleptonic D meson decays have attracted great attention recently. The very different data for the $D^0 \rightarrow \pi^+ \pi^-$ and $D^0 \rightarrow K^+ K^-$ branching ratios have been a long-standing puzzle: the former (latter) is lower (higher) than theoretical predictions from analyses based on the topology parametrization [1,2]. The deviation in these two $D \rightarrow PP$ modes, P representing a pseudoscalar meson, stands even after taking into account flavor $SU(3)$ symmetry breaking effects in emission amplitudes [1]. Another puzzle appears in the difference between the direct CP asymmetries of the $D^0 \rightarrow K^+ K^-$ and $D^0 \rightarrow \pi^+ \pi^-$ decays,

$$\begin{aligned} \Delta A_{CP} &\equiv A_{CP}(K^+ K^-) - A_{CP}(\pi^+ \pi^-) \\ &= [-0.82 \pm 0.21(\text{stat}) \pm 0.11(\text{syst})]\%, \end{aligned} \quad (1)$$

measured by the LHCb Collaboration [3], which is the first evidence of CP violation in charmed meson decays. The above result has been confirmed by the CDF Collaboration [4],¹

$$\Delta A_{CP} = [-0.62 \pm 0.21(\text{stat}) \pm 0.10(\text{syst})]\%. \quad (2)$$

The quantity ΔA_{CP} is naively expected to be much smaller in the Standard Model (SM), since the responsible penguin contributions are suppressed by both the Cabibbo-

Kobayashi-Maskawa (CKM) matrix elements and the Wilson coefficients [6,7],

$$A_{CP} \sim \frac{|V_{cb}^* V_{ub}|}{|V_{cs}^* V_{us}|} \frac{\alpha_s}{\pi} \sim 10^{-4}. \quad (3)$$

The above two puzzles have triggered intensive investigations in the literature employing different approaches. The mechanism responsible for the very different $D^0 \rightarrow \pi^+ \pi^-$ and $D^0 \rightarrow K^+ K^-$ branching ratios is still unclear. It has been speculated that the long-distance resonant contribution through the nearby resonance $f_0(1710)$ in the W -exchange topology could explain why a D^0 meson decays more abundantly to the $K^+ K^-$ than $\pi^+ \pi^-$ final state [1]: it is attributed to the dominance of the scalar glueball content in $f_0(1710)$ and the chiral suppression on the scalar glueball decay into two pseudoscalar mesons. This mechanism was systematically formulated in the single pole-dominance model with additional arbitrary ‘‘Wilson coefficients,’’ and then included in the topology parametrization for global fits [8]. Unfortunately, the predicted $D^0 \rightarrow \pi^+ \pi^-$ ($D^0 \rightarrow K^+ K^-$) branching ratio remains higher (lower) than the data. That is, a systematic and global understanding of the $D \rightarrow PP$ decays has not existed yet. Because of the high precision of the two data, even a small deviation deteriorates the global fit. If the branching ratios are not well explained, some important decay mechanism may still be missing, and any predictions for the direct CP asymmetries are not convincing.

¹The CDF Collaboration observed the smaller direct CP asymmetries $A_{CP}(D^0 \rightarrow \pi^+ \pi^-) = (+0.22 \pm 0.24 \pm 0.11)\%$ and $A_{CP}(D^0 \rightarrow K^+ K^-) = (-0.24 \pm 0.22 \pm 0.09)\%$ in [5].

For the second puzzle, a reliable evaluation of the penguin contributions to two-body nonleptonic D meson decays is not available so far. In [9,10] the tree amplitudes were determined by fitting the topology parametrization to the data of the branching ratios, while the penguin amplitudes were calculated in the QCD-improved factorization (QCDF) [11,12]. That is, the tree and penguin contributions were treated in the different theoretical frameworks. It has been noticed that the penguin amplitudes derived from QCDF lead to a tiny ΔA_{CP} of order 10^{-5} [10]. Allowing the penguin amplitudes to be of the same order as the tree ones discretionally, ΔA_{CP} reaches $-0.13\% \sim O(10^{-3})$ [10]. In another work [13] also based on the topology parametrization, the penguin contribution via an internal b quark was identified as the major source of CP violation, since it cannot be related to the tree amplitudes. This penguin contribution, including its strong phase, was constrained by the LHCb data and then adopted to predict direct CP asymmetries of other decay modes. In this way it is difficult to tell whether the large $\Delta A_{CP} \sim O(10^{-2})$ in Eqs. (1) and (2) arise from new physics [14–20]. The similar comment applies to the analysis in [21]. Viewing the postulated ΔA_{CP} ranges from 10^{-5} to 10^{-2} in the SM [22], it is crucial to give precise predictions for the direct CP asymmetries in the $D \rightarrow PP$ decays.

In this paper we aim at proposing a theoretical framework, in which various contributions, such as emission and annihilation ones, and tree and penguin ones, are all handled consistently. The only assumption involved is the factorization of short-distance dynamics and long-distance dynamics in two-body nonleptonic D meson decays into Wilson coefficients and hadronic matrix elements of four-fermion operators, respectively. For the hadronic matrix elements, including the emission, W -annihilation, and W -exchange amplitudes, the treatment is similar to the topology parametrization in the factorization hypothesis. The quark-loop and magnetic-penguin contributions are absorbed into the Wilson coefficients for the penguin operators. As to the scale of the Wilson coefficients, we set it to the energy release in individual decay modes, which depends on masses of final states. An important ingredient is the Glauber strong phase factor [23] associated with a pion, whose strength has been constrained by the data of the $B \rightarrow \pi K$ direct CP asymmetries [24]. Briefly speaking, we have improved the topology parametrization by taking into account mode-dependent QCD dynamics, for instance, flavor $SU(3)$ symmetry breaking effects, in two-body nonleptonic D meson decays.

Because of the small charm quark mass $m_c \approx 1.3$ GeV, a perturbative theory may not be valid for D meson decays. However, with the abundant data, all the above hadronic parameters can be determined. It will be shown that the Glauber phase associated with a pion is crucial for understanding the $D^0 \rightarrow \pi^+ \pi^-$ branching ratio very different from the $D^0 \rightarrow K^+ K^-$ one. This additional phase modifies

the relative angle and the interference between the emission and annihilation amplitudes involving pions. The predicted $D^0 \rightarrow \pi^+ \pi^-$ branching ratio is then reduced, while the predicted $D^+ \rightarrow \pi^+ \eta$ branching ratio is enhanced, such that the overall agreement with the data is greatly improved. Our scale choice for the Wilson coefficients impacts the $D \rightarrow PP$ decays containing the η' meson in the final states: the η' meson mass about 1 GeV is not negligible compared to the D meson mass, so the energy release in these modes should be lower. Once the hadronic parameters are fixed by the measured branching ratios, the penguin amplitudes, expressed as the combination of the hadronic parameters and the corresponding Wilson coefficients, are also fixed in our framework. That is, we can predict the direct CP asymmetries of the $D \rightarrow PP$ decays in the SM without ambiguity. In particular, we obtain $\Delta A_{CP} = -1.00 \times 10^{-3}$, which discriminates the opposite postulations on large (small) direct CP asymmetries in singly Cabibbo-suppressed D meson decays [25] ([26]). It will be observed that the quark loops and the scalar penguin annihilation generate large relative phases between the tree and penguin amplitudes, and are the dominant sources of the direct CP asymmetries.

In Sec. II we present our parametrization of the tree contributions to the $D \rightarrow PP$ branching ratios based on the factorization hypothesis with QCD dynamics being implemented. In Sec. III the penguin contributions from the operators O_{3-6} , from $O_{1,2}$ through the quark loops, and from the magnetic penguin O_{8g} are formulated. The direct CP asymmetries in the $D \rightarrow PP$ decays are then predicted. Section IV is the conclusion. We show the explicit topology parametrization for the $D^0 \rightarrow \pi^+ \pi^-$ and $D^0 \rightarrow K^+ K^-$ decays in Appendix A. Appendix B collects the evolution formulas for the Wilson coefficients in the scale μ . The η - η' mixing formalism and the chiral factors of their flavor states are given in Appendix C. The form factors involved in the factorizable scalar penguin annihilation are specified in Appendix D.

II. BRANCHING RATIOS

In this section we formulate the tree contributions, which dominate the branching ratios of charm decays. The relevant weak effective Hamiltonian is written as

$$\mathcal{H}_{\text{eff}} = \frac{G_F}{\sqrt{2}} V_{\text{CKM}} [C_1(\mu) O_1(\mu) + C_2(\mu) O_2(\mu)] + \text{H.c.}, \quad (4)$$

where G_F is the Fermi coupling constant, V_{CKM} denotes the corresponding CKM matrix elements, $C_{1,2}$ are the Wilson coefficients, and the current-current operators are

$$\begin{aligned} O_1 &= (\bar{u}_\alpha q_{2\beta})_{V-A} (\bar{q}_{1\beta} c_\alpha)_{V-A}, \\ O_2 &= (\bar{u}_\alpha q_{2\alpha})_{V-A} (\bar{q}_{1\beta} c_\beta)_{V-A}, \end{aligned} \quad (5)$$

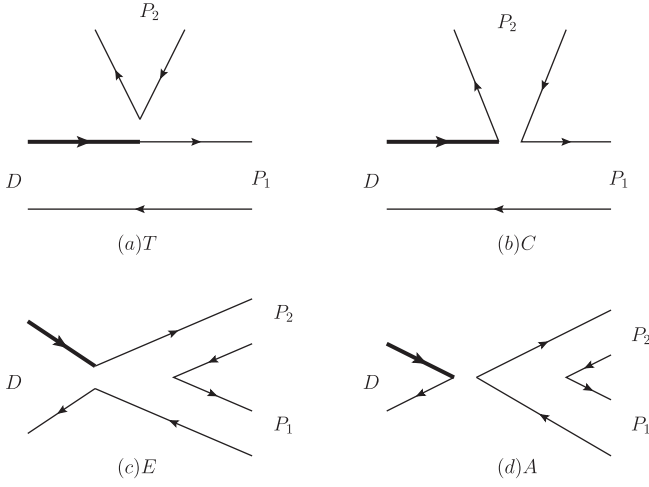


FIG. 1. Four topological diagrams contributing to $D \rightarrow PP$ decays: (a) the color-favored tree amplitude T , (b) the color-suppressed tree amplitude C , (c) the W -exchange amplitude E , and (d) the W -annihilation amplitude A . The thick line represents the charm quark.

with α, β being color indices, and $q_{1,2}$ being the d or s quark. There are four types of topologies dominantly contributing to the branching ratios of $D \rightarrow P_1 P_2$ decays [27], where P_2 represents the meson emitted from the weak vertex: the color-favored tree amplitude T , the color-suppressed amplitude C , the W -exchange amplitude E , and the W -annihilation amplitude A , shown in Fig. 1. Penguin contributions are neglected for branching ratios due to the suppression of the CKM matrix elements $V_{cb}^* V_{ub}$. Besides, there exist flavor-singlet amplitudes, in which a quark-antiquark pair produced from vacuum generates color- and flavor-singlet states like $\eta^{(\prime)}$. However, they are also neglected in this work, since the current data do not suggest significant flavor-singlet contributions [1,2].

It is known that the heavy quark expansion does not work well for charm decays because of the small m_c , so that nonfactorizable contributions, such as vertex corrections, final-state interaction (FSI), and resonance effects, cannot be ignored, especially in the amplitude C . We parametrize these contributions into a factor χ_{nf} . For simplicity, we drop nonfactorizable contributions in the amplitude T , which is dominated by factorizable ones. In general, there exists a relative strong phase ϕ between T and C , which may arise from inelastic FSI or other long-distance dynamics in D meson decays [1,8]. Therefore, the emission amplitudes T and C are parametrized as

$$\langle P_1 P_2 | \mathcal{H}_{\text{eff}} | D \rangle_{T,C} = \frac{G_F}{\sqrt{2}} V_{\text{CKM}} a_{1,2}(\mu) f_{P_2} (m_D^2 - m_{P_1}^2) \times F_0^{DP_1}(m_{P_2}^2), \quad (6)$$

with the P_1 (P_2) meson mass m_{P_1} (m_{P_2}), the P_2 meson decay constant f_{P_2} , and the $D \rightarrow P_1$ transition form factor

$F_0^{DP_1}$. The scale-dependent Wilson coefficients are given by

$$a_1(\mu) = C_2(\mu) + \frac{C_1(\mu)}{N_c}, \quad (7)$$

$$a_2(\mu) = C_1(\mu) + C_2(\mu) \left[\frac{1}{N_c} + \chi_{nf} e^{i\phi} \right],$$

for T and C , respectively, with $N_c = 3$ being the number of colors.

The flavor $SU(3)$ symmetry breaking effects have been known to be significant in the $D \rightarrow PP$ decays, especially in the singly Cabibbo-suppressed modes [1,8,28]. In addition to the different decay constants f_{P_2} and form factors $F_0^{DP_1}$, the mass ratios $m_{K, \eta^{(\prime)}}/m_D$ should be distinguished too, with m_K , $m_{\eta^{(\prime)}}$, and m_D being the masses of the kaon, the $\eta^{(\prime)}$ meson, and the D meson, respectively. As suggested in the perturbative QCD (PQCD) approach [29], the scale μ is set to the energy release in individual decay processes, which depends on final-state masses. We propose the choice

$$\mu = \sqrt{\Lambda m_D (1 - r_2)}, \quad (8)$$

where $r_2 = m_{P_2}^2/m_D^2$ is the mass ratio of the P_2 meson over the D meson, and Λ , representing the momentum of soft degrees of freedom in the D meson, is a free parameter. The evolution of the Wilson coefficients in the scale μ is shown in Appendix B. The above choice further takes into account the $SU(3)$ breaking effect in the Wilson coefficients for the emission amplitudes. It is then legitimate to regard χ_{nf} , ϕ , and Λ as being universal to all modes, which will be determined by experimental data.

The $D^0 \rightarrow K^0 \bar{K}^0$ branching ratio through the pure W -exchange channel vanishes in the $SU(3)$ limit due to the cancellation of the CKM matrix elements [1,30]. Hence, the large observed branching ratio of this mode manifests the breaking of the flavor $SU(3)$ symmetry in the W -exchange contribution, which becomes almost of the same order as the emission one. Both the W -exchange topology for neutral D meson decays and the W -annihilation topology for charged D meson decays will be included in our framework. Since the factorizable contributions to these amplitudes are down by the helicity suppression, we consider only the nonfactorizable contributions. Then the former (latter) is proportional to the Wilson coefficient C_2 (C_1). Based on the above reasoning, we parametrize the amplitudes E and A as

$$\langle P_1 P_2 | \mathcal{H}_{\text{eff}} | D \rangle_{E,A} = \frac{G_F}{\sqrt{2}} V_{\text{CKM}} b_{q,s}^{E,A}(\mu) f_D m_D^2 \left(\frac{f_{P_1} f_{P_2}}{f_\pi^2} \right), \quad (9)$$

with the factors

$$b_{q,s}^E(\mu) = C_2(\mu)\chi_{q,s}^E e^{i\phi_{q,s}^E}, \quad b_{q,s}^A(\mu) = C_1(\mu)\chi_{q,s}^A e^{i\phi_{q,s}^A}. \quad (10)$$

The dimensionless parameters $\chi_{q,s}^{E,A}$ and $\phi_{q,s}^{E,A}$ describe the strengths and the strong phases of the involved matrix elements, where the superscripts q, s differentiate the light quarks and the strange quarks strongly produced in pairs. The b 's are defined for the $\pi\pi$ final states, to which those for other final states are related via the ratio of the decay constants $f_{P_1} f_{P_2} / f_\pi^2$. That is, the flavor $SU(3)$ breaking effects from the strongly produced quark pairs and from the decay constants have been taken into account. The parameters $\chi_{q,s}^{E,A}$ and $\phi_{q,s}^{E,A}$ are then assumed to be universal and will be determined from data. Similarly, we consider the $SU(3)$ breaking effect in the energy release, which defines the scale of the Wilson coefficients $C_{1,2}(\mu)$

$$\mu = \sqrt{\Lambda m_D (1 - r_1^2)(1 - r_2^2)}, \quad (11)$$

with the mass ratios $r_{1,2} = m_{P_1, P_2} / m_D$.

As pointed out in [24], a special type of soft gluons, called the Glauber gluons, may introduce an additional strong phase to a nonfactorizable amplitude in two-body heavy-meson decays. The Glauber phase associated with a pion is more significant, because of its simultaneous role as a Nambu-Goldstone boson and a $q\bar{q}$ bound state: the valence quark and antiquark of the pion are separated by a short distance in order to reduce the confinement potential energy, while the multiparton states of the pion spread over a huge space-time in order to meet the role of a massless Nambu-Goldstone boson [31]. The relatively larger soft effect from the multiparton states in the pion results in the Glauber phase. Hence, we assign a phase factor $\exp(iS_\pi)$ for each pion involved in the nonfactorizable amplitudes E and A . The phase factor associated with the $\pi\pi$ final states is then given by $\exp(2iS_\pi)$ as explicitly shown in Appendix A. The reason we do not introduce the Glauber phase into the nonfactorizable emission diagrams but only into the W -exchange and W -annihilation diagrams is that the emission topology mainly receives factorizable contributions in most of the decay modes. Since the Glauber phase appears only in nonfactorizable amplitudes, we will not include it in the emission topology in the present work.

In summary, our parametrization for the emission amplitudes in Eq. (6) and the W -exchange and W -annihilation ones in Eq. (9) contains 12 free parameters. The global fit to all the data of 28 $D \rightarrow PP$ branching ratios leads to the outcomes

$$\begin{aligned} \Lambda &= 0.56 \text{ GeV}, & \chi_{nf} &= -0.59, & \chi_q^E &= 0.11, \\ \chi_s^E &= 0.18, & \chi_q^A &= 0.12, & \chi_s^A &= 0.17, \\ S_\pi &= -0.50, & \phi &= -0.62, & \phi_q^E &= 4.80, \\ \phi_s^E &= 4.23, & \phi_q^A &= 4.06, & \phi_s^A &= 3.48, \end{aligned} \quad (12)$$

with the fitted $\chi^2 = 6.9$ per degree of freedom, which marks a great improvement compared to $\chi^2 = 87$ in [1]. The parameter $\Lambda = 0.56$ GeV indeed corresponds to the soft momentum involved in the D meson, implying the typical energy release $\mu \sim 1$ GeV. This scale, which is not very low, indicates that the PQCD factorization formulas [32] might provide a useful guideline for formulating various contributions to the $D \rightarrow PP$ decays in our framework. Since the fermion flows of the amplitudes E and A can be converted into each other through the Fierz transformation, the relations $\chi_q^E \sim \chi_q^A$, $\chi_s^E \sim \chi_s^A$, and the similar relations for the strong phases are expected. The satisfactory fit also confirms our postulation that the helicity suppression works well, and the nonfactorizable contributions dominate the W -exchange and W -annihilation amplitudes. A large $SU(3)$ breaking effect has been revealed by the inequality $\chi_q^{E(A)} \neq \chi_s^{E(A)}$. The values in Eq. (12) support $E > A$ in [1,8] according to Eq. (10), consistent with the fact that the D^0 meson lifetime is shorter than the D^+ meson lifetime. The Glauber phase $S_\pi = -0.50$ is in agreement with that extracted in [24], which resolves the puzzle from the dramatically different data for the direct CP asymmetries $A_{CP}(B^0 \rightarrow \pi^\mp K^\pm)$ and $A_{CP}(B^\pm \rightarrow \pi^0 K^\pm)$.

Our results for the $D \rightarrow PP$ branching ratios are presented in Tables I, II, and III for the Cabibbo-favored, singly Cabibbo-suppressed, and doubly Cabibbo-suppressed decays, respectively. The experimental data, as well as the predictions from other approaches, such as the topological-diagram approach [1], the factorization approach combined with the pole-dominant model for the W -exchange and W -annihilation contributions [8], and an analysis with FSI effects from nearby resonances [26], are also listed for comparison. It is obvious that the predictions for the singly Cabibbo-suppressed decays, including the $D^0 \rightarrow \pi^+ \pi^-$, $K^+ K^-$, and $K^0 \bar{K}^0$ modes, are consistent with the data: the known large $SU(3)$ breaking effects in these decays have been properly described in our parametrization. The major sources to χ^2 of our fit come from the $D^0 \rightarrow \pi^0 \pi^0$ ($\Delta\chi^2 = 23$) and $D^+ \rightarrow \pi^+ \pi^0$ ($\Delta\chi^2 = 17$) decays. These modes are exceptional in the sense that they involve the color-suppressed emission amplitudes C , which are dominated by the nonfactorizable contributions. To reduce χ^2 , more $SU(3)$ breaking effects, such as the Glauber phase in C [24], need to be introduced.

The Wilson coefficients for the $D^0 \rightarrow \pi^+ \pi^-$ and $K^+ K^-$ decays,

$$\begin{aligned} a_1(\pi\pi) &= 1.09, & a_2(\pi\pi) &= 0.81e^{i147.8^\circ}, \\ a_1(KK) &= 1.10, & a_2(KK) &= 0.83e^{i148.2^\circ}, \end{aligned} \quad (13)$$

similar to those obtained in [1,8], and

$$C_2(\pi\pi) = 1.26, \quad C_2(KK) = 1.27, \quad (14)$$

for the W -exchange and W -annihilation amplitudes indicate minor $SU(3)$ breaking effects from the scale running.

TABLE I. Branching ratios in units of percentages for Cabibbo-favored $D \rightarrow PP$ decays. Our results are compared to those from the analysis including FSI effects [26], the topological-diagram approach [1], the pole-dominant model [8], and the experimental data [33].

Modes	Br(FSI)	Br(diagram)	Br(pole)	Br(exp)	Br(this work)
$D^0 \rightarrow \pi^0 \bar{K}^0$	1.35	2.36 ± 0.08	2.4 ± 0.7	2.38 ± 0.09	2.41
$D^0 \rightarrow \pi^+ K^-$	4.03	3.91 ± 0.17	3.9 ± 1.0	3.891 ± 0.077	3.70
$D^0 \rightarrow \bar{K}^0 \eta$	0.80	0.98 ± 0.05	0.8 ± 0.2	0.96 ± 0.06	1.00
$D^0 \rightarrow \bar{K}^0 \eta'$	1.51	1.91 ± 0.09	1.9 ± 0.3	1.90 ± 0.11	1.73
$D^+ \rightarrow \pi^+ \bar{K}^0$	2.51	3.08 ± 0.36	3.1 ± 2.0	3.074 ± 0.096	3.22
$D_S^+ \rightarrow K^+ \bar{K}^0$	4.79	2.97 ± 0.32	3.0 ± 0.9	2.98 ± 0.08	3.00
$D_S^+ \rightarrow \pi^+ \eta$	1.33	1.82 ± 0.32	1.9 ± 0.5	1.84 ± 0.15	1.65
$D_S^+ \rightarrow \pi^+ \eta'$	5.89	3.82 ± 0.36	4.6 ± 0.6	3.95 ± 0.34	3.44
$D_S^+ \rightarrow \pi^+ \pi^0$		0	0	<0.06	0

TABLE II. Same as Table I except for singly Cabibbo-suppressed $D \rightarrow PP$ decays in units of 10^{-3} .

Modes	Br(FSI)	Br(diagram)	Br(pole)	Br(exp)	Br(this work)
$D^0 \rightarrow \pi^+ \pi^-$	1.59	2.24 ± 0.10	2.2 ± 0.5	1.45 ± 0.05	1.43
$D^0 \rightarrow K^+ K^-$	4.56	1.92 ± 0.08	3.0 ± 0.8	4.07 ± 0.10	4.19
$D^0 \rightarrow K^0 \bar{K}^0$	0.93	0	0.3 ± 0.1	0.320 ± 0.038	0.36
$D^0 \rightarrow \pi^0 \pi^0$	1.16	1.35 ± 0.05	0.8 ± 0.2	0.81 ± 0.05	0.57
$D^0 \rightarrow \pi^0 \eta$	0.58	0.75 ± 0.02	1.1 ± 0.3	0.68 ± 0.07	0.94
$D^0 \rightarrow \pi^0 \eta'$	1.7	0.74 ± 0.02	0.6 ± 0.2	0.91 ± 0.13	0.65
$D^0 \rightarrow \eta \eta$	1.0	1.44 ± 0.08	1.3 ± 0.4	1.67 ± 0.18	1.48
$D^0 \rightarrow \eta \eta'$	2.2	1.19 ± 0.07	1.1 ± 0.1	1.05 ± 0.26	1.54
$D^+ \rightarrow \pi^+ \pi^0$	1.7	0.88 ± 0.10	1.0 ± 0.5	1.18 ± 0.07	0.89
$D^+ \rightarrow K^+ \bar{K}^0$	8.6	5.46 ± 0.53	8.4 ± 1.6	6.12 ± 0.22	5.95
$D^+ \rightarrow \pi^+ \eta$	3.6	1.48 ± 0.26	1.6 ± 1.0	3.54 ± 0.21	3.39
$D^+ \rightarrow \pi^+ \eta'$	7.9	3.70 ± 0.37	5.5 ± 0.8	4.68 ± 0.29	4.58
$D_S^+ \rightarrow \pi^0 K^+$	1.6	0.86 ± 0.09	0.5 ± 0.2	0.62 ± 0.23	0.67
$D_S^+ \rightarrow \pi^+ K^0$	4.3	2.73 ± 0.26	2.8 ± 0.6	2.52 ± 0.27	2.21
$D_S^+ \rightarrow K^+ \eta$	2.7	0.78 ± 0.09	0.8 ± 0.5	1.76 ± 0.36	1.00
$D_S^+ \rightarrow K^+ \eta'$	5.2	1.07 ± 0.17	1.4 ± 0.4	1.8 ± 0.5	1.92

TABLE III. Same as Table I except for doubly Cabibbo-suppressed $D \rightarrow PP$ decays in units of 10^{-4} .

Modes	Br(diagram)	Br(pole)	Br(exp)	Br(this work)
$D^0 \rightarrow \pi^0 K^0$	0.67 ± 0.02	0.6 ± 0.2		0.69
$D^0 \rightarrow \pi^- K^+$	1.12 ± 0.05	1.6 ± 0.4	1.48 ± 0.07	1.67
$D^0 \rightarrow K^0 \eta$	0.28 ± 0.02	0.22 ± 0.05		0.29
$D^0 \rightarrow K^0 \eta'$	0.55 ± 0.03	0.5 ± 0.1		0.50
$D^+ \rightarrow \pi^+ K^0$	1.98 ± 0.22	1.7 ± 0.5		2.38
$D^+ \rightarrow \pi^0 K^+$	1.59 ± 0.15	2.2 ± 0.4	1.72 ± 0.19	1.97
$D^+ \rightarrow K^+ \eta$	0.98 ± 0.04	1.2 ± 0.2	1.08 ± 0.17^a	0.66
$D^+ \rightarrow K^+ \eta'$	0.91 ± 0.17	1.0 ± 0.1	1.76 ± 0.22^b	1.14
$D_S^+ \rightarrow K^+ K^0$	0.38 ± 0.04	0.7 ± 0.4		0.63

^aData from [34].

^bData from [34].

As pointed out in [10], to account for the $D^0 \rightarrow \pi^+ \pi^-$ and $D^0 \rightarrow K^+ K^-$ branching ratios, their W -exchange amplitudes must be different in both the magnitudes and the strong phases. In our parametrization, the distinction in the magnitudes is achieved by differentiating χ_q from χ_s and the decay constant f_π from f_K , while the distinction in the strong phases is achieved by the Glauber phase S_π . Another significant improvement appears in the prediction for the $D^+ \rightarrow \pi^+ \eta$ branching ratio as indicated in Table II. The branching ratios obtained in [1,8] are small, because the emission and annihilation amplitudes extracted from the Cabibbo-favored processes lead to a destructive interference in this Cabibbo-suppressed mode. In our framework the additional Glauber phase associated with the pion changes the destructive interference into a constructive one. This provides another support for the $SU(3)$ breaking effect caused by the Glauber phase.

The scale-dependent Wilson coefficients do improve the overall agreement between the theoretical predictions and the data involving the η' meson. Taking the $D^+ \rightarrow \pi^+ \eta'$ decay as an example, the corresponding parameters are given by $a_1(\pi\eta') = 1.12$ and $a_2(\pi\eta') = 0.89e^{i149.6^\circ}$ for the emission amplitudes with the η' meson emitted from the weak vertex, and $C_2(\pi\eta') = 1.32$ for the annihilation amplitudes. Compared to Eqs. (13) and (14), it is clear that the lower energy release involved in the $D^+ \rightarrow \pi^+ \eta'$ decay with heavier final states increases the Wilson coefficients. Benefited from the scale-dependent Wilson coefficients, χ^2 from all the η' involved modes is reduced by nearly 10, relative to χ^2 in the previous fits in the pole model [8].

III. DIRECT CP ASYMMETRIES

In this section we predict the direct CP asymmetries in the $D \rightarrow PP$ decays by combining the short-distance dynamics associated with the penguin operators and the long-distance parameters in Eq. (12). The direct CP asymmetry, defined by

$$A_{CP}(f) = \frac{\Gamma(D \rightarrow f) - \Gamma(\bar{D} \rightarrow \bar{f})}{\Gamma(D \rightarrow f) + \Gamma(\bar{D} \rightarrow \bar{f})}, \quad (15)$$

exists only in singly Cabibbo-suppressed modes.

A. Tree-level CP violation

A $D \rightarrow PP$ mode, receiving contributions proportional to both λ_d and λ_s , has the decay amplitude

$$\mathcal{A} = \lambda_d \mathcal{A}_d + \lambda_s \mathcal{A}_s. \quad (16)$$

The interference between the two terms in \mathcal{A} leads to the tree-level direct CP asymmetry

$$A_{CP} \approx -2 \frac{\text{Im}(\lambda_d^* \lambda_s)}{|\lambda_d|^2} \frac{\text{Im}(\mathcal{A}_d^* \mathcal{A}_s)}{|\mathcal{A}_d - \mathcal{A}_s|^2}, \quad (17)$$

TABLE IV. Direct CP asymmetries in $D \rightarrow PP$ decays in the units of (10^{-3}) . A_{CP}^{tree} denotes the tree-level CP asymmetry and A_{CP}^{tot} denotes the CP asymmetry arising from the interference between the total tree and penguin amplitudes. Results from the analysis, including FSI effects [26], and from the topological-diagram approach [10] are presented for comparison.

Modes	$A_{CP}(\text{FSI})$	$A_{CP}(\text{diagram})$	A_{CP}^{tree}	A_{CP}^{tot}
$D^0 \rightarrow \pi^+ \pi^-$	0.02 ± 0.01	0.86	0	0.58
$D^0 \rightarrow K^+ K^-$	0.13 ± 0.8	-0.48	0	-0.42
$D^0 \rightarrow \pi^0 \pi^0$	-0.54 ± 0.31	0.85	0	0.05
$D^0 \rightarrow K^0 \bar{K}^0$	-0.28 ± 0.16	0	1.11	1.38
$D^0 \rightarrow \pi^0 \eta$	1.43 ± 0.83	-0.16	-0.33	-0.29
$D^0 \rightarrow \pi^0 \eta'$	-0.98 ± 0.47	-0.01	0.53	1.53
$D^0 \rightarrow \eta \eta$	0.50 ± 0.29	-0.71	0.29	0.18
$D^0 \rightarrow \eta \eta'$	0.28 ± 0.16	0.25	-0.30	-0.94
$D^+ \rightarrow \pi^+ \pi^0$		0	0	0
$D^+ \rightarrow K^+ \bar{K}^0$	-0.51 ± 0.30	-0.38	-0.13	-0.93
$D^+ \rightarrow \pi^+ \eta$		-0.65	-0.54	-0.26
$D^+ \rightarrow \pi^+ \eta'$		0.41	0.38	1.18
$D_S^+ \rightarrow \pi^0 K^+$		0.88	0.32	0.39
$D_S^+ \rightarrow \pi^+ K^0$		0.52	0.13	0.84
$D_S^+ \rightarrow K^+ \eta$		-0.19	0.80	0.70
$D_S^+ \rightarrow K^+ \eta'$		-0.41	-0.45	-1.60

where the relation $\lambda_d + \lambda_s \approx 0$ has been inserted into the denominator. Except for the final states with the $\eta^{(\prime)}$ meson, which contains both the $q\bar{q}$ and $s\bar{s}$ components, four other channels $D^0 \rightarrow K^0 \bar{K}^0$, $D^+ \rightarrow K^+ \bar{K}^0$, $D_S^+ \rightarrow \pi^+ K^0$, and $D_S^+ \rightarrow \pi^0 K^+$ also exhibit the tree-level CP violation, though their values have been found to be small [10]. We can predict the tree-level CP violation in the $D^0 \rightarrow K^0 \bar{K}^0$ decay as indicated in Table IV, which is not attainable in the diagrammatic approach in the $SU(3)$ limit [10]. This is one of the advantages of our formalism that has taken into account most of the $SU(3)$ breaking effects. The CP asymmetries in this mode, including the CP violation in the K^0 - \bar{K}^0 mixing, would possibly be measured.

B. Penguin-induced CP violation

We extend our formalism to the penguin contributions to the $D \rightarrow PP$ decays. For this purpose, the effective Hamiltonian for singly Cabibbo-suppressed charm decays,

$$\begin{aligned} \mathcal{H}_{\text{eff}} = & \frac{G_F}{\sqrt{2}} \left[\sum_{q=d,s} V_{cq}^* V_{uq} (C_1(\mu) O_1^q(\mu) + C_2(\mu) O_2^q(\mu)) \right. \\ & \left. - V_{cb}^* V_{ub} \left(\sum_{i=3}^6 C_i(\mu) O_i(\mu) + C_{8g}(\mu) O_{8g}(\mu) \right) \right], \end{aligned} \quad (18)$$

is considered, with the QCD-penguin operators

$$\begin{aligned}
O_3 &= \sum_{q'=u,d,s} (\bar{u}_\alpha c_\alpha)_{V-A} (\bar{q}'_\beta q'_\beta)_{V-A}, \\
O_4 &= \sum_{q'=u,d,s} (\bar{u}_\alpha c_\beta)_{V-A} (\bar{q}'_\beta q'_\alpha)_{V-A}, \\
O_5 &= \sum_{q'=u,d,s} (\bar{u}_\alpha c_\alpha)_{V-A} (\bar{q}'_\beta q'_\beta)_{V+A}, \\
O_6 &= \sum_{q'=u,d,s} (\bar{u}_\alpha c_\beta)_{V-A} (\bar{q}'_\beta q'_\alpha)_{V+A},
\end{aligned} \tag{19}$$

and the chromomagnetic penguin operator,

$$O_{8g} = \frac{g}{8\pi^2} m_c \bar{u} \sigma_{\mu\nu} (1 + \gamma_5) T^a G^{a\mu\nu} c, \tag{20}$$

T^a being a color matrix. The explicit expressions for the Wilson coefficients $C_{3-6}(\mu)$ in terms of the running coupling constant $\alpha_s(\mu)$ are given in Appendix B. Four types of penguin topologies are shown in Fig. 2

Below we sort out the short-distance dynamics associated with the above penguin operators. The contributions from the $(V-A)(V-A)$ current in the operators $O_{3,4}$ can be directly related to those from the tree operators by replacing the Wilson coefficients. The relations between the hadronic matrix elements from the $(V-A)(V+A)$ or $(S+P)(S-P)$ current and from the $(V-A)(V-A)$ current are subtler. For the penguin color-favored emission amplitudes, we have

$$\begin{aligned}
P_T &= a_3(\mu) \langle P_2 | (\bar{q}q)_{V-A} | 0 \rangle \langle P_1 | (\bar{u}c)_{V-A} | D \rangle \\
&\quad + a_5(\mu) \langle P_2 | (\bar{q}q)_{V+A} | 0 \rangle \langle P_1 | (\bar{u}c)_{V-A} | D \rangle, \\
&= [a_3(\mu) - a_5(\mu)] f_{P_2} (m_D^2 - m_{P_1}^2) F_0^{DP_1}(m_{P_2}^2),
\end{aligned} \tag{21}$$

with the Wilson coefficients

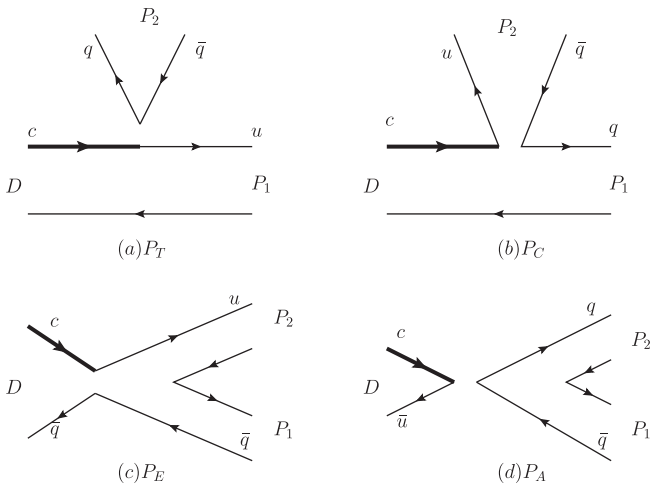


FIG. 2. Four topological penguin diagrams contributing to $D \rightarrow PP$ decays: (a) the penguin color-favored emission amplitude P_T , (b) the penguin color-suppressed emission amplitude P_C , (c) the penguin exchange amplitude P_E , and (d) the penguin annihilation amplitude P_A . Note that $P_T(P_C)$ is not truly color-favored (color-suppressed), but possesses the same topology as $T(C)$.

$$a_3(\mu) = C_3(\mu) + \frac{C_4(\mu)}{N_c}, \quad a_5(\mu) = C_5(\mu) + \frac{C_6(\mu)}{N_c}, \tag{22}$$

where the minus sign in front of the Wilson coefficient a_5 arises from the equality $\langle P_2 | (\bar{q}q)_{V+A} | 0 \rangle = -\langle P_2 | (\bar{q}q)_{V-A} | 0 \rangle$.

We write the penguin color-suppressed emission amplitude as

$$\begin{aligned}
P_C &= a_4(\mu) \langle P_2 | (\bar{u}q)_{V-A} | 0 \rangle \langle P_1 | (\bar{q}c)_{V-A} | D \rangle \\
&\quad - 2a_6(\mu) \langle P_2 | (\bar{u}q)_{S+P} | 0 \rangle \langle P_1 | (\bar{q}c)_{S-P} | D \rangle \\
&= [a_4(\mu) + a_6(\mu) r_\chi] f_{P_2} (m_D^2 - m_{P_1}^2) F_0^{DP_1}(m_{P_2}^2),
\end{aligned} \tag{23}$$

with the Wilson coefficients

$$\begin{aligned}
a_4(\mu) &= C_4(\mu) + C_3(\mu) \left[\frac{1}{N_c} + \chi_{nf} e^{i\phi} \right], \\
a_6(\mu) &= C_6(\mu) + C_5(\mu) \left[\frac{1}{N_c} + \chi_{nf} e^{i\phi} \right].
\end{aligned} \tag{24}$$

The chiral factor

$$r_\chi = \frac{2m_{P_2}^2}{m_c(m_u + m_q)}, \tag{25}$$

with the u -quark (q -quark) mass m_u (m_q), exhibits formal suppression by a power of $1/m_c$, but takes a value of order unity actually. Note that the $(S-P)(S+P)$ nonfactorizable amplitude cannot be simply related to the $(V-A) \times (V-A)$ nonfactorizable amplitude. However, the PQCD factorization formulas for heavy-meson decays [32] reveal strong similarity between them in the dominant small parton momentum region, which supports the parametrization in Eq. (24). The chiral factor for the $\eta^{(\prime)}$ meson receives an additional contribution from the axial anomaly, as illustrated in Appendix C.

The treatment of the penguin exchange amplitude P_E and the penguin annihilation amplitude P_A demands a more careful formulation. It is obvious that the matrix elements of the operator O_3 (O_4) are similar to those of O_2 (O_1). As discussed in Sec. II, the factorizable contributions to the above matrix elements vanish in the $SU(3)$ limit because of the helicity suppression and have been neglected. Considering only the nonfactorizable contributions, O_4 gives rise to part of P_A . The operator O_6 also contributes to P_A , to which the helicity suppression applies. Therefore, its matrix elements can be combined with those of O_4 under the equality

$$\begin{aligned}
&\langle P_1(q\bar{q}') P_2(q'\bar{q}) | (\bar{u}c)_{V-A} (\bar{q}'q')_{V+A} | D(c\bar{u}) \rangle \\
&= \langle P_1(q\bar{q}') P_2(q'\bar{q}) | (\bar{u}c)_{V-A} (\bar{q}'q')_{V-A} | D(c\bar{u}) \rangle,
\end{aligned} \tag{26}$$

which has been verified by the PQCD factorization formulas [32]. Equation (26) is attributed to the fact that only the vector piece V in the $(\bar{q}'q')_{V\pm A}$ currents contributes to

the production of two pseudoscalar mesons. Thus the QCD-penguin annihilation amplitude is parametrized as

$$P_A = [C_4(\mu) + C_6(\mu)]\chi_{q,s}^A e^{i\phi_{q,s}^A} f_D m_D^2 \left(\frac{f_{P_1} f_{P_2}}{f_\pi^2} \right). \quad (27)$$

For the amplitude P_E , the helicity suppression does not apply to the matrix elements of $O_{5,6}$, so the factorizable contributions exist. The nonfactorizable contribution from O_5 vanishes in the $SU(3)$ limit, as verified by the PQCD factorization formulas [32], and will be neglected. We then apply the Fierz transformation and the factorization hypothesis to

$$\begin{aligned} & \langle P_1(q'\bar{q})P_2(u\bar{q}') | (\bar{u}c)_{V-A} (\bar{q}'q')_{V+A} | D(c\bar{q}) \rangle \\ &= -2 \langle P_1(q'\bar{q})P_2(u\bar{q}') | (\bar{u}q')_{S+P} | 0 \rangle \langle 0 | (\bar{q}'c)_{S-P} | D(c\bar{q}) \rangle. \end{aligned} \quad (28)$$

The scalar form factor involved in the matrix element $\langle P_1(q'\bar{q})P_2(u\bar{q}') | (\bar{u}q')_{S+P} | 0 \rangle$ has been assumed to be dominated by scalar resonances, and fixed in [35]. It has been demonstrated that the similar formalism works for the analysis of the $\tau \rightarrow K\pi\nu_\tau$ decay [35]. Combining the nonfactorizable contribution from O_3 , P_E is written as

$$\begin{aligned} P_E &= C_3(\mu)\chi_{q,s}^E e^{i\phi_{q,s}^E} f_D m_D^2 \left(\frac{f_{P_1} f_{P_2}}{f_\pi^2} \right) \\ &+ 2 \left[C_6(\mu) + \frac{C_5(\mu)}{N_c} \right] g_S B_S(m_D^2) m_S \bar{f}_S f_D \frac{m_D^2}{m_c}, \end{aligned} \quad (29)$$

where g_S is an effective strong coupling constant, \bar{f}_S and m_S are the decay constant and the mass of the scalar resonance particle S , respectively, and the function B_S represents the Breit-Wigner propagator of the scalar resonance,

$$B_S(q^2) = \frac{1}{q^2 - m_S^2 + im_S \Gamma_S(q^2)}. \quad (30)$$

In the above expression q^2 denotes the invariant mass squared of the $P_1 P_2$ final state, and the strong phase from the width $\Gamma_S(q^2)$ provides a major source to direct CP asymmetries. More detail for the treatment of the scalar matrix element $\langle P_1(q'\bar{q})P_2(u\bar{q}') | \bar{u}q' | 0 \rangle$ can be found in Appendix D.

C. Quark loops and magnetic penguin

To complete the penguin contributions to the $D \rightarrow PP$ decays, we include the quark loops from the tree operators and the magnetic penguin as displayed in Fig. 3. The former up to next-to-leading order in the coupling constant can be absorbed into the Wilson coefficients [11]

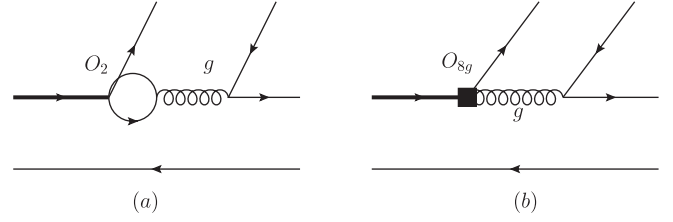


FIG. 3. Quark-loop and magnetic-penguin contributions to $D \rightarrow PP$ decays.

$$C_{3,5}(\mu) \rightarrow C_{3,5}(\mu) - \frac{\alpha_s(\mu)}{8\pi N_c} \sum_{q=d,s} \frac{\lambda_q}{\lambda_b} C^{(q)}(\mu, \langle l^2 \rangle), \quad (31)$$

$$C_{4,6}(\mu) \rightarrow C_{4,6}(\mu) + \frac{\alpha_s(\mu)}{8\pi} \sum_{q=d,s} \frac{\lambda_q}{\lambda_b} C^{(q)}(\mu, \langle l^2 \rangle),$$

with $\langle l^2 \rangle$ being the averaged invariant mass squared of the virtual gluon emitted from the quark loop. The function $C^{(q)}$ is written as

$$C^{(q)}(\mu, \langle l^2 \rangle) = \left[G^{(q)}(\mu, \langle l^2 \rangle) - \frac{2}{3} \right] C_2(\mu), \quad (32)$$

with the function

$$G^{(q)}(\mu, \langle l^2 \rangle) = -4 \int_0^1 dx x(1-x) \ln \frac{m_q^2 - x(1-x)\langle l^2 \rangle}{\mu^2}. \quad (33)$$

Because of the smallness of the associated CKM matrix elements, we have ignored the quark loops from the penguin operators.

Using the unitarity relation of the CKM matrix, we reexpress the second term in Eq. (31) as

$$\frac{\alpha_s(\mu)}{8\pi} \frac{\lambda_d C^{(d)} + \lambda_s C^{(s)}}{\lambda_b} = \frac{\alpha_s(\mu)}{8\pi} \left[\frac{\lambda_d}{\lambda_b} (C^{(d)} - C^{(s)}) - C^{(s)} \right]. \quad (34)$$

The term proportional to λ_d contributes to the tree amplitudes, which is, however, numerically negligible, $(\alpha_s/8)\pi(C^{(d)} - C^{(s)}) \sim O(10^{-4}) \ll C_{1,2}$. It is the reason we did not include the quark loops in the analysis of the branching ratios. Keeping only the second term in Eqs. (34) and (31) reduces to

$$C_{3,5}(\mu) \rightarrow C_{3,5}(\mu) + \frac{\alpha_s(\mu)}{8\pi N_c} C^{(s)}(\mu, \langle l^2 \rangle), \quad (35)$$

$$C_{4,6}(\mu) \rightarrow C_{4,6}(\mu) - \frac{\alpha_s(\mu)}{8\pi} C^{(s)}(\mu, \langle l^2 \rangle).$$

We have confirmed that not much numerical difference arises from replacing $C^{(s)}$ by $C^{(d)}$.

The magnetic-penguin contribution can be included in the Wilson coefficients for the penguin operators following the substitutions [11]

$$C_{3,5}(\mu) \rightarrow C_{3,5}(\mu) + \frac{\alpha_s(\mu)}{8\pi N_c} \frac{2m_c^2}{\langle l^2 \rangle} C_{8g}^{\text{eff}}(\mu), \quad (36)$$

$$C_{4,6}(\mu) \rightarrow C_{4,6}(\mu) - \frac{\alpha_s(\mu)}{8\pi} \frac{2m_c^2}{\langle l^2 \rangle} C_{8g}^{\text{eff}}(\mu),$$

with the effective Wilson coefficient $C_{8g}^{\text{eff}} = C_{8g} + C_5$. To predict the direct CP asymmetries, we adopt $\langle l^2 \rangle \approx (P_1/2 + P_2/2)^2 \approx m_D^2/4$. This choice of $\langle l^2 \rangle$ corresponds to the kinematic configuration, where the spectator in the decay takes half of the P_1 meson momentum, consistent with the scale parametrization in Eq. (8), and a valence quark in the P_2 meson also carries half of its momentum. We have varied $\langle l^2 \rangle$ between $m_D^2/2$ and $m_D^2/10$, and observed only a slight change in our predictions for the direct CP asymmetries. The contribution from the magnetic penguin is much smaller than that from the quark loops, $C_{8g}^{\text{eff}} \ll C^{(q)}(\mu, \langle l^2 \rangle)$. It turns out that the integral in Eq. (33) generates a large imaginary part as $m_q^2 \ll \langle l^2 \rangle$ and a sizable shift of the strong phases in the penguin amplitudes.

It is seen that all the important penguin amplitudes have been formulated without introducing additional free parameters. Compared with [9], the similarity is that the effective Wilson coefficients in Eqs. (35) and (36) have been employed. The difference appears in the derivation of the involved hadronic matrix elements. Both the leading-power and subleading-power penguin contributions, including their strengths and strong phases, are determined in our formalism. The leading-power penguin contributions were calculated in QCDF, but the subleading-power ones were estimated in the large N_c assumption in [9]. This is the reason why only the strengths of the penguin contributions were obtained in [9].

D. Numerical results

We adopt $m_u = m_d = \bar{m}_q = 5.3$ MeV and $m_s = 136$ MeV for the quark masses at the scale 1 GeV in the numerical analysis. The inputs for the involved decay constants and transition form factors are taken to be the same as in [8]. In most modes P_C , which is enhanced by the chiral factor, and P_E from the $(S - P)(S + P)$ current are the major QCD-penguin amplitudes. Our predictions for the direct CP asymmetries in the $D \rightarrow PP$ decays are listed in Table IV, which differ from those derived in other approaches, and can be confronted with future data. The result for $D^0 \rightarrow K^0 \bar{K}^0$ is dominated by the tree-level CP violation, because of smallness of the involved penguin annihilation contribution. If considering the isospin symmetry breaking from unequal u and d quark masses, the chiral factors for the $u\bar{u}$ and $d\bar{d}$ components of the π^0 meson will be different. The corresponding penguin contributions then do not cancel exactly, and a nonzero direct CP asymmetry would appear in the $D^+ \rightarrow \pi^+ \pi^0$ decay. If turning off the Glauber phase in the $D^0 \rightarrow \pi^+ \pi^-$ decay,

the direct CP asymmetry $A_{CP}^{\text{tot}}(\pi^+ \pi^-)$ decreases from 0.58×10^{-3} to 0.49×10^{-3} . The 30% change in the branching ratio (see Table II) and the 15% change in the direct CP asymmetry indicate that the Glauber phase is not a negligible mechanism.

We predict the difference between the direct CP asymmetries in the $D^0 \rightarrow K^+ K^-$ and $D^0 \rightarrow \pi^+ \pi^-$ decays,

$$\Delta A_{CP} = -1.00 \times 10^{-3}, \quad (37)$$

which is in the same sign as the data, but an order of magnitude smaller than the central value of the LHCb data in Eq. (1), and lower than the CDF data in Eq. (2). To check whether our prediction makes sense, we write ΔA_{CP} as

$$\Delta A_{CP} = -2r \sin \gamma \left(\frac{|\mathcal{P}^{KK}|}{|\mathcal{T}^{KK}|} \sin \delta^{KK} + \frac{|\mathcal{P}^{\pi\pi}|}{|\mathcal{T}^{\pi\pi}|} \sin \delta^{\pi\pi} \right), \quad (38)$$

with $r = |\lambda_b|/|\lambda_d| = |\lambda_b|/|\lambda_s|$, $\lambda_q = V_{cq}^* V_{uq}$, γ being the CP violating weak phase, and δ^{KK} ($\delta^{\pi\pi}$) being the relative strong phase between the tree amplitude \mathcal{T}^{KK} ($\mathcal{T}^{\pi\pi}$) and the penguin amplitude \mathcal{P}^{KK} ($\mathcal{P}^{\pi\pi}$) for the $D^0 \rightarrow K^+ K^-$ ($D^0 \rightarrow \pi^+ \pi^-$) mode. It is easy to find $r \approx 0.7 \times 10^{-3}$ and $\gamma = (73_{-25}^{+22})^\circ$ from the Particle Data Group 2010 [36], i.e., $2r \sin \gamma \approx 1.3 \times 10^{-3}$. For $|\mathcal{P}|/|\mathcal{T}| \sim O(1)$ and $\sin \delta \sim 1$, ΔA_{CP} could reach only a few times of 10^{-3} . The topological amplitudes for the $D^0 \rightarrow \pi^+ \pi^-$ and $K^+ K^-$ modes obtained in this work are given, in units of 10^{-6} GeV, by

$$T^{\pi\pi} = 2.73, \quad E^{\pi\pi} = 0.82e^{-i142^\circ}, \quad (39)$$

$$T^{KK} = 3.65, \quad E^{KK} = 1.2e^{-i85^\circ},$$

$$P_C^{\pi\pi} = 0.87e^{i134^\circ}, \quad P_E^{\pi\pi} = 0.81e^{i111^\circ},$$

$$P_A^{\pi\pi} = 0.25e^{-i43^\circ}, \quad P_C^{KK} = 1.21e^{i135^\circ}, \quad (40)$$

$$P_E^{KK} = 0.87e^{i111^\circ}, \quad P_A^{KK} = 0.45e^{-i5^\circ},$$

which lead to the total tree and penguin amplitudes and their ratios

$$\mathcal{T}^{\pi\pi} = 2.14e^{-i14^\circ}, \quad \mathcal{P}^{\pi\pi} = 1.40e^{i121^\circ},$$

$$\frac{\mathcal{P}^{\pi\pi}}{\mathcal{T}^{\pi\pi}} = 0.66e^{i134^\circ}, \quad \mathcal{T}^{KK} = 3.94e^{-i18^\circ}, \quad (41)$$

$$\mathcal{P}^{KK} = 1.79e^{i114^\circ}, \quad \frac{\mathcal{P}^{KK}}{\mathcal{T}^{KK}} = 0.45e^{i131^\circ}.$$

It is a concern for our formalism whether all the important nonperturbative sources in D meson decays have been identified. If not, the simple replacement of the Wilson coefficients may not work for estimating the penguin contributions. As explained in the previous section, the outcomes in Eq. (12) are all reasonable, so most of the important nonperturbative sources should have been taken into account. The uncertainty of our formalism arises mainly from the parametrization of the scalar form factors

in P_E . The difference of the direct CP asymmetries changes from -1.0×10^{-3} to -1.6×10^{-3} , when the effective strong coupling $g_S = g_{K^*K\pi}$ is increased by a factor of 2. If varying the strong phases in the penguin amplitudes arbitrarily, ΔA_{CP} would be at most -1.4×10^{-3} . Varying the input parameters, such as the quark masses $\bar{m}_q = 4.0\text{--}6.5$ MeV and $m_s = 108\text{--}176$ MeV, the mass $M_{f_0(1370)} = 1200\text{--}1500$ MeV, and the width $\Gamma_{f_0(1370)} = 200\text{--}500$ MeV of the dominant scalar resonance $f_0(1370)$, and the CKM matrix elements $|V_{ub}| = (3.89 \pm 0.44) \times 10^{-3}$ and $\gamma = (73_{-25}^{+22})^\circ$, we have $\Delta A_{CP} = (-0.57\text{--} - 1.87) \times 10^{-3}$. In conclusion, if the central values of the LHCb and CDF data persist, they can be regarded as a signal of new physics. At this moment, there is plenty of room for accommodating the LHCb and CDF data by means of models extended beyond the SM. Those models with additional sources of CP violation are all suitable candidates, like supersymmetry models, left-right models, models with the leptoquark, the fourth generation, or the diquark, and so on. New-physics effects on the direct CP asymmetries in $D \rightarrow PP$ decays can be explored by combining corresponding short-distance Wilson coefficients with the long-distance parameters determined in this work.

IV. CONCLUSION

In this paper we have proposed a theoretical framework for analyzing two-body nonleptonic D meson decays, based on the factorization of short-distance (long-distance) dynamics into Wilson coefficients (hadronic matrix elements of four-fermion operators). Because of the small charm quark mass just above 1 GeV, a perturbative theory for the hadronic matrix elements may not be valid. Our idea is to identify as completely as possible the important sources of nonperturbative dynamics in the decay amplitudes and parametrize them in the framework of the factorization hypothesis: we have considered the evolution of the Wilson coefficients with the energy release in individual decay modes, which depends on the scale Λ of the soft degrees of freedom in the D meson. The hadronic matrix elements of the four-fermion operators have been parametrized into the strengths χ 's and the strong phases ϕ 's. It is crucial to introduce the Glauber strong phase S_π associated with a pion in the nonfactorizable annihilation amplitudes, which is due to the unique role of the pion as a Nambu-Goldstone boson and a quark-antiquark bound state simultaneously. The flavor $SU(3)$ symmetry breaking effects have been taken into account in the above framework appropriately. Fitting our parametrization to the abundant data of the $D \rightarrow PP$ branching ratios, all the nonperturbative parameters have been determined.

It has been shown that our framework greatly improves the global fit to the measured $D \rightarrow PP$ branching ratios: the evolution of the Wilson coefficients improves the overall agreement with the data involving the η' meson, and the

Glauber phase resolves the long-standing puzzle from the $D^0 \rightarrow \pi^+\pi^-$ and $D^0 \rightarrow K^+K^-$ branching ratios. The Glauber phase has also enhanced the predicted $D^+ \rightarrow \pi^+\eta$ branching ratio, giving much better consistency with the data. The value of Λ is in the correct order of magnitude for characterizing the soft degrees of freedom in the D meson, and the Glauber phase S_π agrees with that extracted from the data for the direct CP asymmetries in the $B \rightarrow \pi K$ decays. The similarity of the χ values for the W exchange and for the W annihilation confirms our expectation, because these two topologies can be converted to each other via the Fierz transformation. The difference between the χ values for the strongly produced light-quark and strange-quark pairs implies the significant $SU(3)$ breaking effects in the $D \rightarrow PP$ decays.

Once having determined the nonperturbative parameters from the fit to the branching ratios, the replacement of the Wilson coefficients works for estimating the penguin contributions. For those penguin amplitudes, which cannot be related to tree amplitudes through the above replacement, we have shown that they are either factorizable or suppressed by the helicity conservation. If they are factorizable, such as the scalar penguin annihilation contribution, data from other processes can be used for their determination. We are then able to predict the direct CP asymmetries in $D \rightarrow PP$ decays without ambiguity. It has been found that the strong phases from the quark loops and the scalar penguin annihilation dominate the direct CP asymmetries. Many of our predictions in Table IV can be confronted with future data. In particular, we have predicted $\Delta A_{CP} = -1.00 \times 10^{-3}$, which is lower than the LHCb and CDF data. As pointed out at the end of the previous section, the uncertainty of our formalism arises mainly from the parametrization of the scalar form factors in P_E . However, even increasing the associated effective strong coupling by a factor of 2, ΔA_{CP} remains of order 10^{-3} . We conclude that the LHCb and CDF data will reveal a new-physics signal, if their central values persist.

ACKNOWLEDGMENTS

We are grateful to Hai-Yang Cheng, Emi Kou, Satoshi Mishima, Nejc Kosnik, Svjetlana Fajfer, and Andrey Tayduganov for useful discussions. This work was supported in part by the National Science Council of R. O. C. under Grant No. NSC-98-2112-M-001-015-MY3, by the National Center for Theoretical Sciences, and by National Science Foundation of China under the Grant No. 11075168.

APPENDIX A: AMPLITUDES

Different decay modes receive contributions from different topological amplitudes. Take the $D^0 \rightarrow \pi^+\pi^-$ and $D^0 \rightarrow K^+K^-$ modes as examples, whose expressions are given by

$$\begin{aligned}
\mathcal{A}(D^0 \rightarrow \pi^+ \pi^-) &= \frac{G_F}{\sqrt{2}} [\lambda_d(T + E) - \lambda_b(P_C + 2P_A^d + P_E^d)], \\
&= \frac{G_F}{\sqrt{2}} \{V_{cd}^* V_{ud} [a_1(\mu)(m_D^2 - m_\pi^2) f_\pi F_0^{D\pi}(m_\pi^2) + C_2(\mu) e^{i(\phi_q^E + 2S_\pi)} \chi_q^E f_D m_D^2] \\
&\quad - V_{cb}^* V_{ub} [a_{P_C}(\mu)(m_D^2 - m_\pi^2) f_\pi F_0^{D\pi}(m_\pi^2) + 2a_{P_A}(\mu) e^{i(\phi_q^A + 2S_\pi)} \chi_q^A f_D m_D^2 + C_3(\mu) e^{i(\phi_q^E + 2S_\pi)} \chi_q^E f_D m_D^2] \\
&\quad + 2a'_6(\mu) g_S f_D \frac{m_D^2}{m_c} \sum_{f_0} B_{f_0}(m_D^2) m_{f_0} \bar{f}_{f_0} \}, \\
\mathcal{A}(D^0 \rightarrow K^+ K^-) &= \frac{G_F}{\sqrt{2}} [\lambda_s(T + E) - \lambda_b(P_C + P_A^u + P_A^s + P_E^s)], \\
&= \frac{G_F}{\sqrt{2}} \left\{ V_{cs}^* V_{us} \left[a_1(\mu)(m_D^2 - m_K^2) f_K F_0^{DK}(m_K^2) + C_2(\mu) e^{i\phi_q^E} \chi_q^E f_D m_D^2 \frac{f_K^2}{f_\pi^2} \right] \right. \\
&\quad - V_{cb}^* V_{ub} \left[a_{P_C}(\mu)(m_D^2 - m_K^2) f_K F_0^{DK}(m_K^2) + a_{P_A}(\mu) e^{i\phi_q^A} \chi_q^A f_D m_D^2 \frac{f_K^2}{f_\pi^2} + a_{P_A}(\mu) e^{i\phi_s^A} \chi_s^A f_D m_D^2 \frac{f_K^2}{f_\pi^2} \right. \\
&\quad \left. \left. + C_3(\mu) e^{i\phi_s^E} \chi_s^E f_D m_D^2 \frac{f_K^2}{f_\pi^2} + 2a'_6(\mu) g_S f_D \frac{m_D^2}{m_c} \sum_{f_0} B_{f_0}(m_D^2) m_{f_0} \bar{f}_{f_0} \right] \right\}, \tag{A1}
\end{aligned}$$

with the coefficients

$$a_{P_C}(\mu) = [a_4(\mu) + a_6(\mu) r_\chi], \quad a_{P_A}(\mu) = C_4(\mu) + C_6(\mu), \quad a'_6(\mu) = C_6(\mu) + \frac{C_5(\mu)}{N_c}. \tag{A2}$$

Notice the Glauber phase factors e^{i2S_π} associated with the nonfactorizable amplitudes χ_q^E and χ_q^A in Eq. (A1).

APPENDIX B: WILSON COEFFICIENTS

In this Appendix we present the evolution of the Wilson coefficients in the scale $\mu < m_c$ [37],

$$C_1(\mu) = 0.2334\alpha^{1.444} + 0.0459\alpha^{0.7778} - 1.313\alpha^{0.4444} + 0.3041\alpha^{-0.2222}, \tag{B1}$$

$$C_2(\mu) = -0.2334\alpha^{1.444} + 0.0459\alpha^{0.7778} + 1.313\alpha^{0.4444} + 0.3041\alpha^{-0.2222}, \tag{B2}$$

$$\begin{aligned}
C_3(\mu) &= 0.0496\alpha^{-0.2977} - 0.0608\alpha^{-0.2222} + 0.0025\alpha^{-0.1196} - 1.23\alpha^{0.4173} + 1.313\alpha^{0.4444} - 0.0184\alpha^{0.7023} \\
&\quad - 0.0076\alpha^{0.7778} - 0.0188\alpha^{0.8025} + 0.0018\alpha^{0.8804} + 0.2362\alpha^{1.417} - 0.1986\alpha^{1.444} + 0.0004\alpha^{1.802}, \tag{B3}
\end{aligned}$$

$$\begin{aligned}
C_4(\mu) &= 0.075\alpha^{-0.2977} - 0.0608\alpha^{-0.2222} + 0.0012\alpha^{-0.1196} + 1.179\alpha^{0.4173} - 1.313\alpha^{0.4444} + 0.0175\alpha^{0.7023} \\
&\quad - 0.014\alpha^{0.7778} + 0.0267\alpha^{0.8025} + 0.0006\alpha^{0.8804} - 0.1807\alpha^{1.417} + 0.129\alpha^{1.444} - 0.002\alpha^{1.802}, \tag{B4}
\end{aligned}$$

$$\begin{aligned}
C_5(\mu) &= -0.0252\alpha^{-0.2977} + 0.0227\alpha^{-0.1196} + 0.0309\alpha^{0.4173} + 0.0251\alpha^{0.7023} + 0.0016\alpha^{0.7778} - 0.0045\alpha^{0.8025} \\
&\quad - 0.0058\alpha^{0.8804} - 0.0338\alpha^{1.417} + 0.0348\alpha^{1.444} - 0.026\alpha^{1.802}, \tag{B5}
\end{aligned}$$

$$\begin{aligned}
C_6(\mu) &= 0.019\alpha^{-0.2977} - 0.0081\alpha^{-0.1196} + 0.0821\alpha^{0.4173} - 0.0624\alpha^{0.7023} - 0.0048\alpha^{0.7778} - 0.1241\alpha^{0.8025} \\
&\quad - 0.0038\alpha^{0.8804} + 0.0979\alpha^{1.417} - 0.1045\alpha^{1.444} - 0.0486\alpha^{1.802}, \tag{B6}
\end{aligned}$$

in terms of the running coupling constant

$$\alpha = \alpha_s(\mu) = \frac{4\pi}{\beta_0 \ln(\mu^2/\Lambda_{\overline{\text{MS}}}^2)} \left[1 - \frac{\beta_1}{\beta_0^2} \frac{\ln \ln(\mu^2/\Lambda_{\overline{\text{MS}}}^2)}{\ln(\mu^2/\Lambda_{\overline{\text{MS}}}^2)} \right], \tag{B7}$$

with the coefficients

$$\beta_0 = \frac{33 - 2f}{3}, \quad \beta_1 = 102 - \frac{38}{3}N_f. \quad (\text{B8})$$

For the active flavor number $N_f = 3$ and the QCD scale $\Lambda_{\overline{\text{MS}}} = \Lambda_{\overline{\text{MS}}}^{(3)} = 375 \text{ MeV}$, we have $\alpha_s(m_c) = 0.407$. The initial conditions of the Wilson coefficients at $\mu = m_c$ are given, in the naïve dimensional regularization scheme, by

$$\begin{aligned} C_1(m_c) &= -0.43, & C_2(m_c) &= 1.22, \\ C_3(m_c) &= 0.018, & C_4(m_c) &= -0.046, \\ C_5(m_c) &= 0.013, & C_6(m_c) &= -0.044. \end{aligned} \quad (\text{B9})$$

Another useful set of values contains

$$\begin{aligned} C_1(1 \text{ GeV}) &= -0.51, & C_2(1 \text{ GeV}) &= 1.27, \\ C_3(1 \text{ GeV}) &= 0.028, & C_4(1 \text{ GeV}) &= -0.065, \\ C_5(1 \text{ GeV}) &= 0.021, & C_6(1 \text{ GeV}) &= -0.058, \end{aligned} \quad (\text{B10})$$

which are evaluated at the typical energy release in two-body nonleptonic D meson decays.

The effective Wilson coefficient C_{8g}^{eff} for the magnetic-penguin operator is known only to the leading-logarithm accuracy. Because of its smallness, we shall not consider the evolution of $C_{8g}^{\text{eff}}(\mu)$, but approximate it by the constant

$$C_{8g}^{\text{eff}}(m_c) = -0.11. \quad (\text{B11})$$

APPENDIX C: CHIRAL FACTOR

The chiral factor in Eq. (25) comes from the relation between the matrix elements of the scalar (pseudoscalar) current and of the vector (axial vector) current. Using the equations of motion, we derive

$$\langle P_2 | \bar{u} \gamma_5 q | 0 \rangle = \frac{-i \partial^\mu \langle P_2 | \bar{u} \gamma_\mu \gamma_5 q | 0 \rangle}{m_u + m_q} = -i \frac{f_{P_2} m_{P_2}^2}{m_u + m_q}, \quad (\text{C1})$$

$$\langle P_1 | \bar{q} c | D \rangle = \frac{-i \partial^\mu \langle P_1 | \bar{q} \gamma_\mu c | 0 \rangle}{m_c} = \frac{m_D^2 - m_{P_1}^2}{m_c} F_0^{DP_1}(m_{P_1}^2), \quad (\text{C2})$$

where the light-quark mass has been neglected in the second expression.

For the $\eta^{(l)}$ meson, the chiral factor receives an additional contribution from the axial anomaly in the following equation of motion: [38]

$$\partial^\mu (\bar{q} \gamma_\mu \gamma_5 q) = 2m_q (\bar{q} i \gamma_5 q) + \frac{\alpha_s}{4\pi} G \tilde{G}, \quad (\text{C3})$$

in which G represents the gluon field tensor, \tilde{G} is its dual, and q denotes the quark fields u , d , and s . In the present analysis only the u quark contributes to the amplitude P_C . We express the physical states η and η' as the linear combinations of the flavor states η_q and η_s via a mixing angle ϕ ,

$$\begin{pmatrix} \eta \\ \eta' \end{pmatrix} = \begin{pmatrix} \cos \phi & -\sin \phi \\ \sin \phi & \cos \phi \end{pmatrix} \begin{pmatrix} \eta_q \\ \eta_s \end{pmatrix}. \quad (\text{C4})$$

The KLOE Collaboration has extracted the value $\phi = (40.4 \pm 0.6)^\circ$ recently [39], which is consistent with the phenomenological result in [38].

Equations (C3) and (C4) then lead to the matrix elements

$$\begin{aligned} \langle \eta | \bar{u} i \gamma_5 u | 0 \rangle &= \frac{1}{2m_u} \left(\frac{1}{\sqrt{2}} m_\eta^2 f_q \cos \phi - \cos \phi \langle \eta_q | \frac{\alpha_s}{4\pi} G \tilde{G} | 0 \rangle \right. \\ &\quad \left. + \sin \phi \langle \eta_s | \frac{\alpha_s}{4\pi} G \tilde{G} | 0 \rangle \right), \end{aligned} \quad (\text{C5})$$

$$\begin{aligned} \langle \eta' | \bar{u} i \gamma_5 u | 0 \rangle &= \frac{1}{2m_u} \left(\frac{1}{\sqrt{2}} m_\eta^2 f_q \sin \phi - \sin \phi \langle \eta_q | \frac{\alpha_s}{4\pi} G \tilde{G} | 0 \rangle \right. \\ &\quad \left. - \cos \phi \langle \eta_s | \frac{\alpha_s}{4\pi} G \tilde{G} | 0 \rangle \right), \end{aligned} \quad (\text{C6})$$

with the η_q decay constant f_q . For the expressions of the anomalies

$$\langle \eta_q | \frac{\alpha_s}{4\pi} G \tilde{G} | 0 \rangle = \sqrt{2} f_q a^2, \quad \langle \eta_s | \frac{\alpha_s}{4\pi} G \tilde{G} | 0 \rangle = y f_q a^2, \quad (\text{C7})$$

the involved parameters have been determined to be $f_q = 1.07 f_\pi$, $a^2 = 0.265 \text{ GeV}^2$, and $y = 0.81$ [38].

APPENDIX D: SCALAR MATRIX ELEMENTS

In this Appendix we fix the scalar matrix element $\langle P_1 P_2 | \bar{q}_1 q_2 | 0 \rangle$ appearing in Sec. III C, which is dominated by the contribution from the lowest scalar resonance [35],

$$\langle P_1 P_2 | \bar{q}_1 q_2 | 0 \rangle = \langle P_1 P_2 | S \rangle \langle S | \bar{q}_1 q_2 | 0 \rangle = g_S B_S(q^2) m_S \tilde{f}_S, \quad (\text{D1})$$

as shown in Eq. (30). The scalar decay constant \tilde{f}_S is defined via $\langle S | \bar{q}_2 q_1 | 0 \rangle = m_S \tilde{f}_S$ [40]. Many scalar mesons have been observed. It is still controversial whether the lightest scalar nonets with the mass smaller than or close to 1 GeV are primarily the four-quark or two-quark bound states. Since κ , $a_0(980)$, and $f_0(980)$ may be the four-quark states, we consider the scalar resonances $a_0(1450)$ for the $\pi\eta$, $\pi\eta'$, and $(KK)^\pm$ final states, $f_0(1370)$, $f_0(1500)$, and $f_0(1710)$ for the $\pi^0\pi^0$, $\pi^+\pi^-$, $K^0\bar{K}^0$, K^+K^- , and $\eta\eta^{(l)}$ final states, and $K_0^*(1430)$ for the $K\pi$ and $K\eta^{(l)}$ final states due to the symmetries of strong interaction. $f_0(1370)$, $f_0(1500)$, and $f_0(1710)$ are the mixtures of $n\bar{n} \equiv (u\bar{u} + d\bar{d})/\sqrt{2}$, $s\bar{s}$, and glueball, but there still exists controversy on the components of each scalar meson. We employ the mixing matrix obtained in [41] in this work. Note that there are no s -wave isospin-1 resonances for the $\pi^\pm\pi^0$ system under the isospin symmetry.

We derive $\langle K\pi | \bar{s}u | 0 \rangle$ as an example. Inserting $K_0^*(1430)$ as the intermediate resonance, the matrix element is written as

$$\begin{aligned} \langle K\pi|\bar{s}u|0\rangle &= \langle K\pi|K_0^*(1430)\rangle\langle K_0^*(1430)|\bar{s}u|0\rangle \\ &= g_{K_0^*K\pi}B_{K_0^*}(q^2)m_{K_0^*}\bar{f}_{K_0^*}, \end{aligned} \quad (\text{D2})$$

where the effective strong coupling constant $g_{K_0^*K\pi} = 3.8$ GeV can be obtained directly from the measured $K_0^*(1430) \rightarrow K\pi$ decay [42], and $B_{K_0^*}$ is the $K_0^*(1430)$ propagator in the Breit-Wigner form [35]

$$B_{K_0^*}(q^2) = \frac{1}{q^2 - m_{K_0^*}^2 + im_{K_0^*}\Gamma_{K_0^*}(q^2)}, \quad (\text{D3})$$

with the momentum-dependent width

$$\begin{aligned} \Gamma_{K_0^*}(q^2) &= \Gamma_{K_0^*}D_{K_0^*}(q^2), \quad D_{K_0^*}(q^2) = \frac{m_{K_0^*}}{\sqrt{q^2}} \frac{P_K(q^2)}{P_K(m_{K_0^*}^2)}, \\ P_K(q^2) &= \frac{1}{2\sqrt{q^2}} \lambda^{1/2}(q^2, m_\pi^2, m_K^2), \\ \lambda(x, y, z) &= x^2 + y^2 + z^2 - 2xy - 2yz - 2xz. \end{aligned} \quad (\text{D4})$$

The values of the mass $m_{K_0^*}$ and the decay width $\Gamma_{K_0^*}$ for the scalar resonance $K_0^*(1430)$ are taken from the Particle Data Group 2010 [36].

The relevant scalar decay constants are given, in QCD sum rules, by [40]

$$\begin{aligned} \bar{f}_{n\bar{n}}(1 \text{ GeV}) &= (460 \pm 50) \text{ MeV}, \\ \bar{f}_{s\bar{s}}(1 \text{ GeV}) &= (490 \pm 50) \text{ MeV}, \\ \bar{f}_{K_0^*(1430)}(1 \text{ GeV}) &= (445 \pm 50) \text{ MeV}, \end{aligned} \quad (\text{D5})$$

where $\bar{f}_{n\bar{n}}$ is the scalar decay constant for $a_0(1450)$ and for the $n\bar{n}$ components of the three isosinglet scalars, and $\bar{f}_{s\bar{s}}$ for the $s\bar{s}$ components of the three isosinglet scalars. We assume that the quark, but not glueball, components of scalars dominate the D meson decays. With a lack of experimental data, the effective coupling constant g_S in Eq. (D1) is approximated by $g_S = g_{K_0^*K\pi}$ in the flavor $SU(3)$ limit.

-
- [1] H.-Y. Cheng and C.-W. Chiang, *Phys. Rev. D* **81**, 074021 (2010).
- [2] B. Bhattacharya and J. L. Rosner, *Phys. Rev. D* **81**, 014026 (2010).
- [3] R. Aaij *et al.* (LHCb Collaboration), *Phys. Rev. Lett.* **108**, 111602 (2012); M. Charles (for the LHCb Collaboration), Proc. Sci. EPS-HEP2011 (2011) 163.
- [4] CDF Collaboration, [arXiv:1207.2158](https://arxiv.org/abs/1207.2158).
- [5] T. Aaltonen *et al.* (CDF Collaboration), *Phys. Rev. D* **85**, 012009 (2012).
- [6] Y. Grossman, A. L. Kagan, and Y. Nir, *Phys. Rev. D* **75**, 036008 (2007).
- [7] I. I. Bigi, A. Paul, and S. Recksiegel, *J. High Energy Phys.* **06** (2011) 089.
- [8] F.-S. Yu, X.-X. Wang, and C.-D. Lu, *Phys. Rev. D* **84**, 074019 (2011).
- [9] J. Brod, A. L. Kagan, and J. Zupan, *Phys. Rev. D* **86**, 014023 (2012).
- [10] H.-Y. Cheng and C.-W. Chiang, *Phys. Rev. D* **85**, 034036 (2012).
- [11] M. Beneke, G. Buchalla, M. Neubert, and C. T. Sachrajda, *Phys. Rev. Lett.* **83**, 1914 (1999); *Nucl. Phys.* **B591**, 313 (2000); M. Beneke and M. Neubert, *Nucl. Phys.* **B675**, 333 (2003).
- [12] M. Beneke, G. Buchalla, M. Neubert, and C. T. Sachrajda, *Nucl. Phys.* **B606**, 245 (2001).
- [13] B. Bhattacharya, M. Gronau, and J. L. Rosner, *Phys. Rev. D* **85**, 054014 (2012).
- [14] Y. Hochberg and Y. Nir, *Phys. Rev. Lett.* **108**, 261601 (2012).
- [15] W. Altmannshofer, R. Primulando, C.-T. Yu, and F. Yu, *J. High Energy Phys.* **04** (2012) 049.
- [16] G. Isidori, J. F. Kamenik, Z. Ligeti, and G. Perez, *Phys. Lett. B* **711**, 46 (2012).
- [17] T. Feldmann, S. Nandi, and A. Soni, *J. High Energy Phys.* **06** (2012) 007.
- [18] G. F. Giudice, G. Isidori, and P. Paradisi, *J. High Energy Phys.* **04** (2012) 060.
- [19] C.-H. Chen, C.-Q. Geng, and W. Wang, *Phys. Rev. D* **85**, 077702 (2012).
- [20] A. N. Rozanov and M. I. Vysotsky, [arXiv:1111.6949](https://arxiv.org/abs/1111.6949) [JETP Lett. (to be published)].
- [21] D. Pirtskhalava and P. Uttayarat, *Phys. Lett. B* **712**, 81 (2012).
- [22] E. Franco, S. Mishima, and L. Silvestrini, *J. High Energy Phys.* **05** (2012) 140.
- [23] C.-p. Chang and H.-n. Li, *Eur. Phys. J. C* **71**, 1687 (2011).
- [24] H.-n. Li and S. Mishima, *Phys. Rev. D* **83**, 034023 (2011).
- [25] M. Golden and B. Grinstein, *Phys. Lett. B* **222**, 501 (1989).
- [26] F. Buccella, M. Lusignoli, G. Miele, A. Pugliese, and P. Santorelli, *Phys. Rev. D* **51**, 3478 (1995); F. Buccella, M. Lusignoli, G. Mangano, G. Miele, A. Pugliese, and P. Santorelli, *Phys. Lett. B* **302**, 319 (1993).
- [27] L.-L. Chau, *Phys. Rep.* **95**, 1 (1983); L.-L. Chau and H.-Y. Cheng, *Phys. Rev. Lett.* **56**, 1655 (1986); *Phys. Rev. D* **36**, 137 (1987); M. Gronau, O. F. Hernandez, D. London, and J. L. Rosner, *Phys. Rev. D* **50**, 4529 (1994); **52**, 6374 (1995).
- [28] Y.-L. Wu, M. Zhong, and Y.-F. Zhou, *Eur. Phys. J. C* **42**, 391 (2005).
- [29] Y.-Y. Keum, H.-n. Li, and A. I. Sanda, *Phys. Lett. B* **504**, 6 (2001); *Phys. Rev. D* **63**, 054008 (2001); C.-D. Lu, K. Ukai, and M.-Z. Yang, *Phys. Rev. D* **63**, 074009 (2001); C.-D. Lu and M.-Z. Yang, *Eur. Phys. J. C* **23**, 275 (2002).
- [30] J. O. Eeg, S. Fajfer, and J. Zupan, *Phys. Rev. D* **64**, 034010 (2001).

- [31] G.P. Lepage and S.J. Brodsky, [Phys. Lett. **87B**, 359 \(1979\)](#); S. Nussinov and R. Shrock, [Phys. Rev. D **79**, 016005 \(2009\)](#); M. Duraisamy and A.L. Kagan, [Eur. Phys. J. C **70**, 921 \(2010\)](#).
- [32] H.-n. Li, S. Mishima, and A.I. Sanda, [Phys. Rev. D **72**, 114005 \(2005\)](#).
- [33] H. Mendez *et al.* (CLEO Collaboration), [Phys. Rev. D **81**, 052013 \(2010\)](#).
- [34] E. Won *et al.* (Belle Collaboration), [Phys. Rev. Lett. **107**, 221801 \(2011\)](#).
- [35] S.Y. Choi, J. Lee, and J. Song, [Phys. Lett. B **437**, 191 \(1998\)](#).
- [36] K. Nakamura *et al.* (Particle Data Group Collaboration), [J. Phys. G **37**, 075021 \(2010\)](#).
- [37] S. Fajfer, P. Singer, and J. Zupan, [Eur. Phys. J. C **27**, 201 \(2003\)](#).
- [38] T. Feldmann, P. Kroll, and B. Stech, [Phys. Rev. D **58**, 114006 \(1998\)](#); [Phys. Lett. B **449**, 339 \(1999\)](#).
- [39] F. Ambrosino *et al.*, [J. High Energy Phys. **07** \(2009\) 105](#).
- [40] H.-Y. Cheng, C.-K. Chua, and K.-C. Yang, [Phys. Rev. D **73**, 014017 \(2006\)](#).
- [41] H.-Y. Cheng, C.-K. Chua, and K.-F. Liu, [Phys. Rev. D **74**, 094005 \(2006\)](#).
- [42] S. Fajfer and J. Zupan, [Int. J. Mod. Phys. A **14**, 4161 \(1999\)](#).